Very High Laser Intensities via Resonant Raman Compression

N. J. Fisch[1,2], V. M. Malkin[2], Z. Toroker[1,2]

[1] *Department of Astrophysical Sciences, Princeton University, Princeton, NJ, USA*

[2] *Princeton Plasma Physics Laboratory, Princeton University, Princeton, NJ, USA*

The largest laser intensities to date are achieved through the technique of chirped pulse amplification, which is subject to the material limits of conventional materials. At very high laser intensity and fluence, these materials fail, limiting the intensity of the output pulses. These material limits may be overcome through the use of plasma as a medium mediating resonant backward Raman amplification in plasma, wherein a short counter-propagating seed pulse, with frequency downshifted from a long pump pulse by the plasma frequency, absorbs the pump energy through a resonant decay interaction of the two light waves and a plasma wave.

In the pump-depletion regime, the counter-propagating seed pulse assumes a self-contracting self-similar form, capturing the pump energy in a pulse of far shorter duration [1]. In order to produce the shortest output pulses, or in order to achieve the effect in the uv or soft x-ray regime [2], the highest possible density plasma should be employed. The high density is also useful because the resonant plasma wave has higher phase velocity, thereby making it more immune to both wave-breaking and Landau damping.

However, at high density, the group velocity dispersion must be taken into account, along with the relativistic electron nonlinearity that limits the extent of amplification [3]. Absent any remediation, at high density, the seed pulse would undergo significant group velocity dispersion, limiting the effectiveness of the Raman compression. However, by proper chirping of the seed pulse, the group velocity dispersion may in fact be used to advantage [4]. The seed chirping effect is distinguished from the pump chirping effect in a density gradient, which may be used to eliminate premature backscatter from noise [5] or to avoid deleterious precursors [6]. The two chirping effects may be used simultaneously to achieve the additive advantages of both.

In the case of pump chirping, the chirping is employed in the presence of a density gradient, which gives a gradient to the plasma frequency. The chirping of the pump pulse may be arranged so that a seed at constant frequency would be in Raman resonance as it encounters the pump. The seed encounters a different carrier frequency of the pump as it traverses the plasma, but the local plasma density at these encounter changes as well.

In dense plasma, it is the seed chirping that can play a larger role. To evaluate the chirping effect, the resonant 3-wave equations in cold plasma, in the presence of both group velocity

dispersion and relativistic nonlinearity of the amplified pulse, may be put in the form [7]:

$$a_t + a_z = bf\ , \quad f_t = -ab^*,$$
$$b_t - b_z c_b/c_a = -af^* - i\kappa b_{tt} + iR|b|^2 b. \tag{1}$$

Here a, b and f are envelopes of the pump, seed and Langmuir waves, respectively, normalized such that the input pump amplitude is $a_0 = 1$. For such a normalization, the envelopes of electron quiver velocities in fields a, b and f are caA, $cbA\sqrt{\omega_a/\omega_b}$ and $cfA\sqrt{\omega_a/\omega_e}$, respectively. Here ω_a, ω_b and ω_e satisfy the resonance condition $\omega_a = \omega_b + \omega_e$; while A is the dimensionless vector potential of the input pump pulse, linked to the input pump intensity I_0 in plasma by the formula $A = \sqrt{2I_0\lambda_a/\omega_a}\, e/m_e c^2$, where λ_a is the pump wavelength in plasma, m_e is the electron mass, $-e$ is the electron charge, c is the speed of light in vacuum, and $\omega_e = \sqrt{4\pi n_e e^2/m_e}$ is the plasma frequency. The group velocities of the pump and seed laser pulses in plasma are $c_a = c\sqrt{1-\omega_e^2/\omega_a^2}$ and $c_b = c\sqrt{1-\omega_e^2/\omega_b^2}$. The time t is measured in units of $1/V_3 A$ and the distance z in units of $c_a/V_3 A$, where $V_3 = (k_f c/2)\sqrt{\omega_e/2\omega_b}$ is the 3-wave coupling constant, $k_f = k_a + k_b$ is the resonant Langmuir wavenumber, $k_a = 2\pi/\lambda_a = \sqrt{\omega_a^2 - \omega_e^2}/c$ and $k_b = \sqrt{\omega_b^2 - \omega_e^2}/c$. The cubic nonlinearity and group velocity dispersion coefficients are $R = A\omega_e^2\omega_a/4\omega_b^2 V_3$ and $\kappa = AV_3\omega_e^2/[(\omega_b^2 - \omega_e^2)2\omega_b]$.

Fig. 1 shows an example in which the chirped seed depletes the pump in about half the distance. Here, $\omega_e/\omega_b = 0.57$. The chirp also results in significant *reshaping* of the output seed. Note that the output amplitude and duration of the first spike of the amplified seed in both chirped and non-chirped cases are approximately the same. Since this output is achieved at half the distance (and hence half the pump energy) in the chirped case, clearly chirping advantageously causes a larger fraction of the pump energy to be captured in the main spike [4].

One of the important applications of seed and pump chirping is to overcome non-resonant regions of plasma which may flank a resonant homogeneous section of plasma. This occurs particularly in the case of high-power applications; since the plasma transverse size grows with the power, but the depth does not, and the fall-off in plasma density in the axial direction may then be dominated by the transverse extent.

Suppose then that a homogeneous central section of length z_h is flanked by end sections of length Δ_n of exponentially decaying density. In Fig. 2, we show how seed chirping helps in the case $\Delta_n = 2z_h$. For the non-chirped case, the initial pump intensity is $I_{a0} = 84.55$ PW/cm^2, with $A = 0.0612$; for the chirped case, the initial pump intensity is $I_{a0} = 24$ PW/cm^2. The pump wavelength is $\lambda_a = 0.351\ \mu$m and the plasma density in the homogeneous section is $n_h = 10^{21}$ cm^{-3}. We show the normalized quiver velocities in the pump, seed, and Langmuir waves,

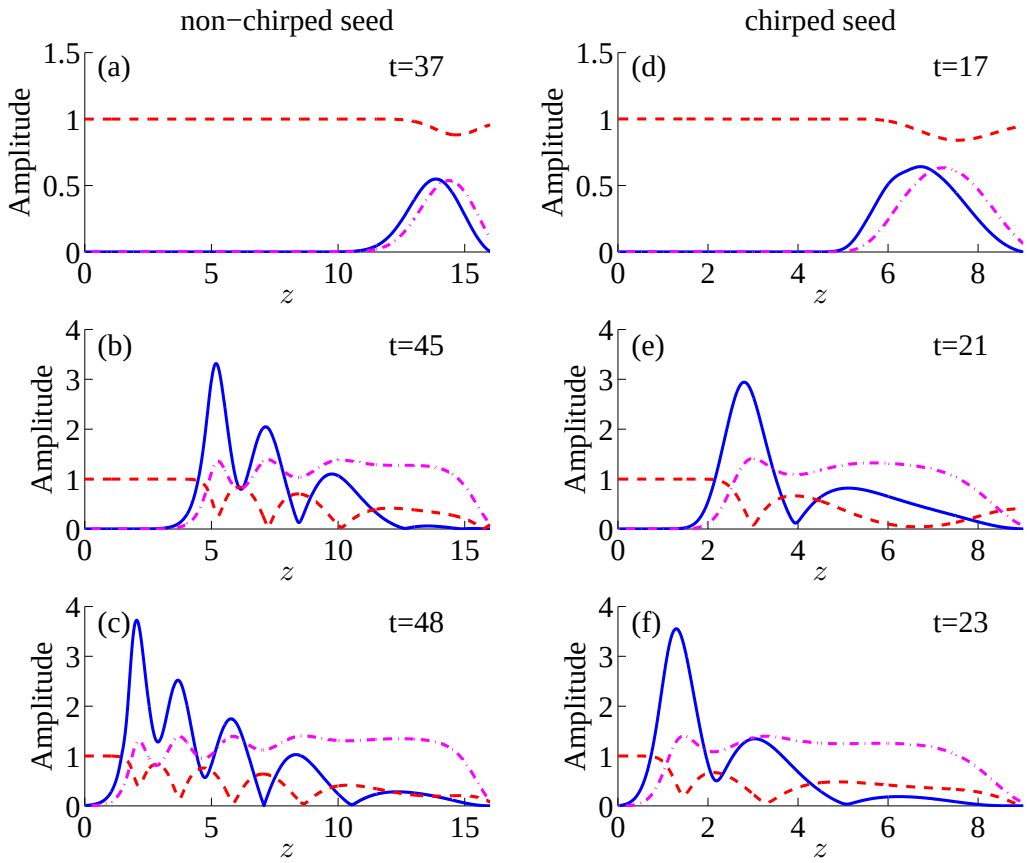

Figure 1: Wave amplitude for non-chirped seed (a, b, and c) and for chirped seed (d, e, and f), for pump , $|a|$, dashed curve; seed , $|b|$, solid curve, and Langmuir wave, $|f|$, dash-dot curve.

defined by $|v_{eh}| = cA\bar{v}_{eh}$, where $\bar{v}_{eh} = |h|\sqrt{\omega_a/\omega_h}$ ($h \in \{a,b,f\}$). In calculating these results, we supplemented Eqs. (1) to evolve the electron temperature [4], including self-consistently the Landau and inverse Bremsstrahlung damping.

For the non chirped pump and seed case (Fig. 2a-c) the Raman compression starts at the right edge (Fig. 2a) and stops at the left edge of the homogeneous section (Fig. 2b), where the seed amplitude is highest and its duration shortest. As the seed exits through the plasma coupler (Fig. 2c), its amplitude decreases. However, by chirping the pump, the resonance condition can be satisfied also in the region where the plasma density is at least half that in the homogeneous section. The initial pump intensity is smaller to avoid wave-breaking in the resonant region where the plasma density is small. But, since the pump chirping enables the Raman compression over a longer plasma length, the amplified seed pulse is larger. Since the non-resonant region over which it propagates is shorter, there is less room for deleterious effects.

The seed chirping is used to obtain the maximum Raman compression within the resonance

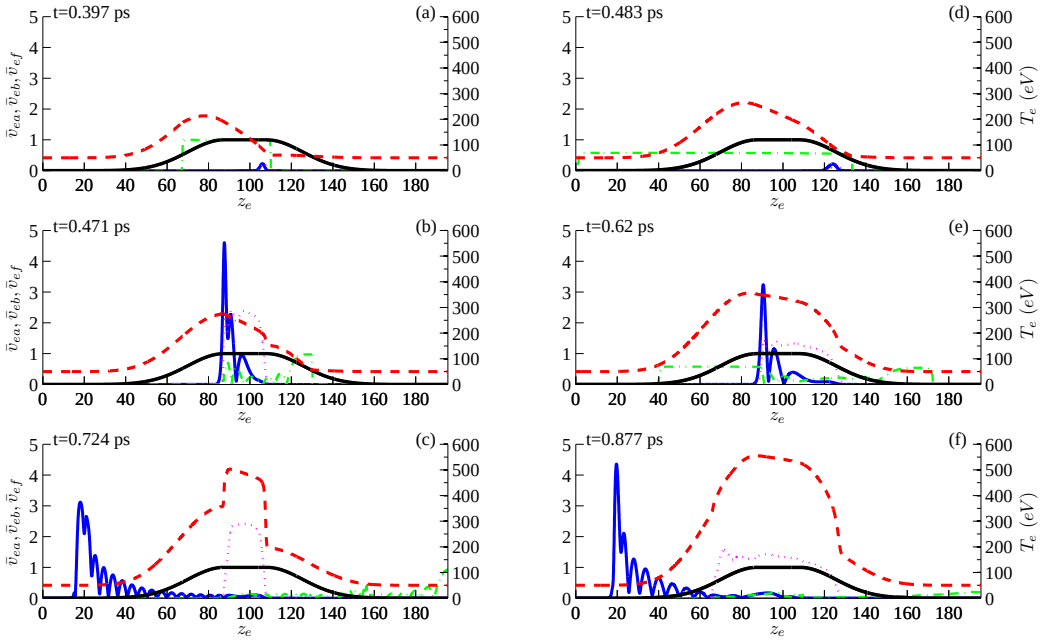

Figure 2: Chirped case (*a-c*) and non-chirped (*d-f*): electron temperature (dashed); quiver velocities for seed, $\bar{v}_{eb}$ (solid); pump, $\bar{v}_{ea}$ (dash-dot); and Langmuir wave, $\bar{v}_{ef}$ (dotted). The solid thick curve is the plasma density profile.

region. As Fig. 2d shows, the initial pump intensity is smaller by a factor of 3.5 and its width longer by 3. Figure 2e shows that the amplified seed pulse at the edge of the homogeneous section. In Fig. 2f, further amplification and compression is evident as the seed traverses the coupler region, since the chirped pump maintains resonance as the density decreases.

Work supported by US DOE and the NNSA.

References

[1] V. M. Malkin, G. Shvets, and N. J. Fisch, Phys. Rev. Lett. **82**, 4448 (1999).

[2] V. M. Malkin, N. J. Fisch, and J. S. Wurtele, Physical Review E **75**, 026404 (2007).

[3] V. M. Malkin, Z. Toroker, and N. J. Fisch, Physics of Plasma **19**, 023109 (February, 2012).

[4] Z. Toroker, V. M. Malkin, and N. J. Fisch, submitted for publication (2012).

[5] V. M. Malkin, G. Shvets, and N. J. Fisch, Phys. Rev. Lett. **84**, 1208 (2000).

[6] Y. A. Tsidulko, V. M. Malkin, and N. J. Fisch, Phys. Rev. Lett. **88**, 235004 (2002).

[7] V. M. Malkin and N. J. Fisch, Phys. Rev. Lett. **99**, 205001 (2007).